ELSEVIER

Journal of Nuclear Materials 241–243 (1997) 456–461

journal of nuclear materials

# Low energy neutral particle fluxes in the JET divertor

R. Reichle [a,*], J.K. Ehrenberg [a], N.A.C. Gottardi [b], L.D. Horton [a], L.C. Ingesson [a], H.J. Jäckel [a], G.K. McCormick [a], A. Loarte [a], R. Simonini [a], M.F. Stamp [a]

[a] *JET Joint Undertaking, Abingdon, Oxfordshire OX14 3EA, UK*

[b] *Commission European Community, DGXVII, E2 Bâtiment Cube, L-2920 Luxembourg, Luxembourg*

**Abstract**

First measurements are presented of the total power loss through neutral particles and their average energy in the JET divertor. The method used distinguishes between the heat flux and the electromagnetic radiation on bolometers. This is done by comparing measurements from inside the divertor either with opposite lines of sight or with a tomographic reconstruction of the radiation. The typical value of the total power loss in the divertor through neutrals is about 1 MW. The average energy of the neutral particles at the inner divertor leg is 1.5–3 eV when detachment is in progress, which agrees with EDGE2D/NIMBUS modelling.

*Keywords:* JET; Divertor plasma; Neutral particle diagnostic; Energy balance

## 1. Introduction

The energy carried from the plasma edge to the wall via low energy neutral particle fluxes, is a difficult but very important quantity to measure. For ITER it has been estimated that the erosion of in-vessel mirrors by neutral particle fluxes may cause more degradation than the neutron damage [1]. The largest fluxes are expected in high pressure divertors.

The measurement of the low energy neutral fluxes usually requires large time-of-flight equipment. Pressure gauges and $D_\alpha$ measurements only give the particle fluxes but no energy information. Bolometers are capable of measuring the heat flux from particles provided it can be distinguished from the electromagnetic heat flux. Here this distinction is made based on the assumptions that most of the neutral particle fluxes stem from the divertor region and that the bulk plasma acts as a shield against neutral particle fluxes for bolometers on the opposite side of the plasma.

## 2. Experimental method

In Fig. 1 the lines of sight are shown which were available for bolometer measurements in the 1994/95 experimental campaign of JET with the Mark I divertor. During this period, only about half of the shown channels could be used at any time. An important detail of the divertor detectors is that they are blackened inside with a carbon layer of a thickness in the micrometer range. This extends the spectral sensitivity range to include also the visible and near ultra-violet part of the spectrum and absorbs most of the energy of the neutrals [5,6].

The anisotropic diffusion model tomography (ADMT) method [7] is applied to reconstruct the radiation distribution with a spatial resolution of 8 cm. For the reconstructions it is assumed that the variation of the radiation perpendicular to the field lines in the poloidal plane is 5 times larger than the variation parallel to them. In the divertor a 5 to 20 times larger spatial variation is assumed than in the bulk.

In this paper the signal in divertor bolometers is separated into contributions from neutrals and light. This is done either by direct comparison with opposite lines of sight or by comparison with tomographic reconstructions

* Corresponding author. Tel.: +44-1235 464 586; fax: +44-1235 464 535; e-mail: rreichle@jet.uk.


*PII* S0022-3115(96)00546-6

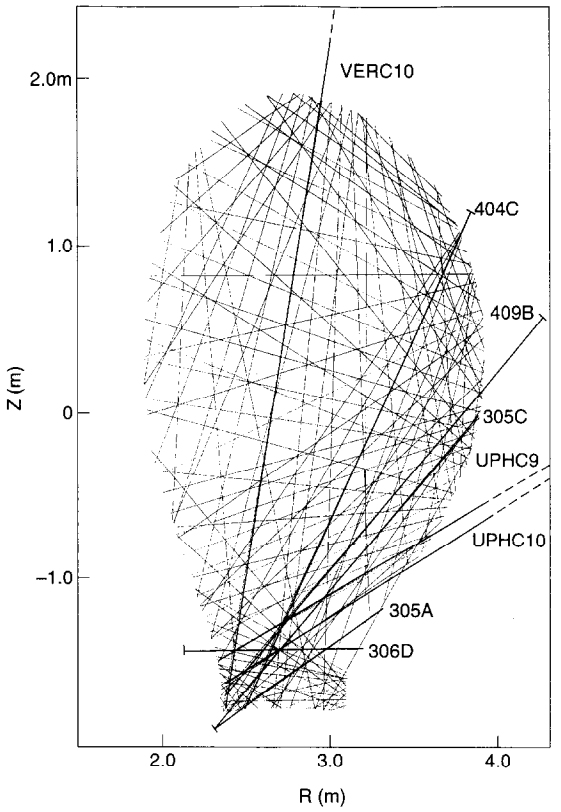


Fig. 1. Lines of sight of bolometers in the Mark I divertor campaign with labels on the ones discussed in detail. VERC10, UPHC9 and UPHC10 belong to the old KB1 bolometer [2]; lines of sight of the new high-temperature in-vessel bolometer [3,4] are 305A, 305C and 306D originating in the divertor, and 404C and 409B, originating in the upper, outer half of the vessel.

using many lines of sight looking at the divertor from outside the divertor volume.

## 3. Experimental results

### 3.1. Moderate heating and only intrinsic impurities

Discharge 31504 is an example where no reconstruction is necessary to see the difference between the measurements from within the divertor and the ones from outside. This is a discharge with 4 MW neutral beam heating, no impurity seeding, and a density ramp up to the density limit (Fig. 2), where a pressure of 0.8 Pa in the divertor is reached. With the density rise the plasma detaches and the radiation moves from the target to the X-point (Fig. 3). In this case data are available for opposite lines of sight, in particular 305C and 409B (see Fig. 1) which are nearly collinear, but also 404C, UPHC10 and VERC10, which look from the outer wall onto the same divertor area as 409B. Fig. 4 shows that 305C, which looks out of the divertor, sees much more signal than 409B, particular during the early attached phase. Noteworthy are the significant intensity oscillations on 305C as the divertor leg is swept with a frequency of 4 Hz across the field of view. This modulation is used to determine details of the radial radiation distribution (Section 5). But as an initial input into an comparison with modelling (Section 4) it shall be assumed that the whole difference between 305C and 409B is due to neutral fluxes, since this is the best way to mimic the tomographic reconstruction, with its present restrictions, i.e. no explicit accountancy for finite solid angles.

### 3.2. Significant heating and seeded impurities

Discharge 33204 is an example of the type of discharge most commonly used to create radiative divertors in the Mark I configuration (Fig. 5). It has 14 MW of neutral beam heating, strong nitrogen seeding and achieves de-

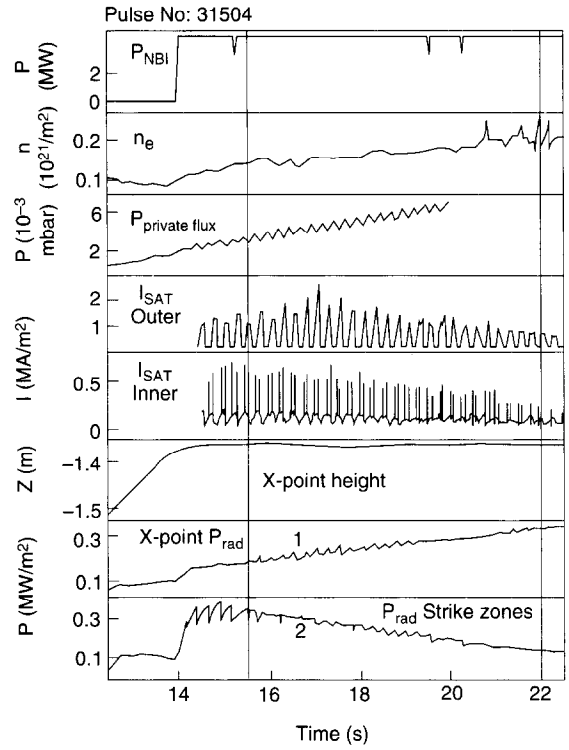


Fig. 2. Overview of discharge 31504: neutral beam power $P_{NBI}$, line integrated electron density $n_e$ from central interferometer cord, neutral pressure in the private flux region $P_{private\ flux}$, ion saturation current at outer and inner strike point $I_{SAT}$, Outer and Inner, vertical position of X-point, line integrated radiation measured by bolometers with a vertical line of sight through the X-point: X-point $P_{rad}$ and a horizontal line of sight just above the target: $P_{rad}$ Strike zones.

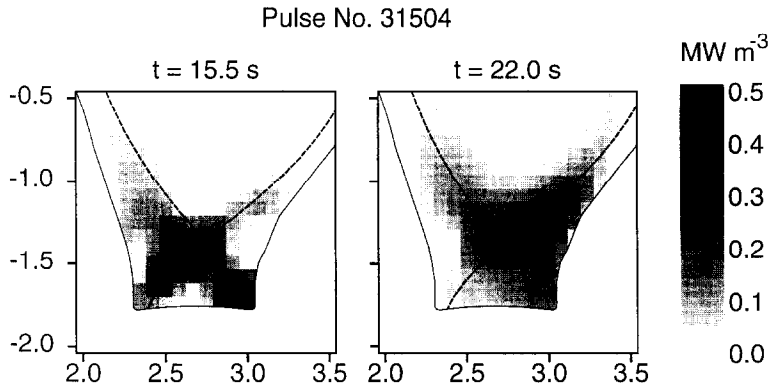


Fig. 3. Tomographic reconstruction of the radiation distribution in the attached (15.5 s) and the detached phase (22.0 s) of discharge 31504.

tachment of the plasma from the target plate when the vertical bolometer, which can not see neutral losses in the divertor, measures about 80% radiated power fraction. Tomographic reconstruction of the radiation taking also the divertor radiation into account gives a good agreement in the total radiated power (Fig. 6). This is not surprising since the largest part of the radiation originates from the seeded impurities and the neutrals can play only a minor part. That there is however nevertheless a noticeable neutral contribution is shown with the trace 305A, which looks out of the inner strike point area of divertor upwards to the outer half, and 306D which looks horizontally across the X-point. 305A is similar to 305C in the previous example. It shows the process of the detachment by its decreasing signal level and the sweep causes the same type of oscillations except that now ELMs are present, which enhance the signal spuriously. At the three times chosen

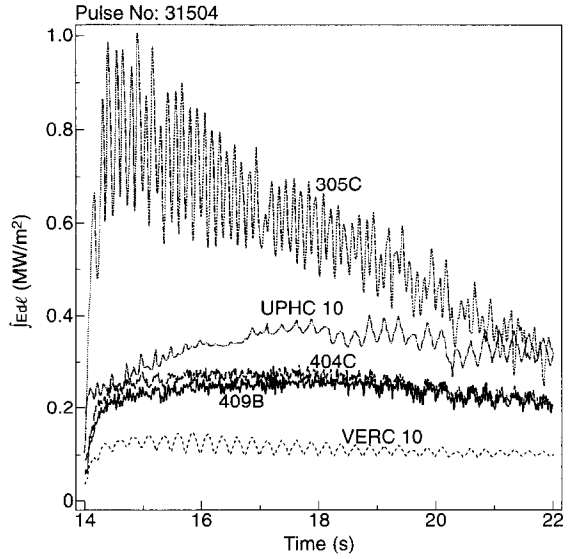


Fig. 4. Line of sight integrals of the radiation from individual bolometers during discharge 31504, see Fig. 1 for identification.

for comparing measurement and reconstruction of 305A, both agree in this example and the total radiation calculated in the reconstructions from all bolometers agrees reasonably well with the one from the vertical lines of KB1 only. At time slices next to the first two chosen ones, but with 305A at its peak, larger mismatches occurred, suggesting that the higher signal levels in 305A are at least partly due to neutral fluxes as well. For 306D a clear discrepancy appears at 19 s. This difference between measurement and reconstruction is evaluated by using results from other plasma parameter measurements.

The total flux of neutral deuterium atoms in the divertor is estimated from $D_\alpha$ and pressure gauge measurements to be $4 \cdot 10^{22}$ D-atoms/s at 19 s. It is assumed that the neutrals emerge isotropically from the main emission area just above the X-point due to its MARFE character [3] (Fig. 5b). As a first step, this area is approximated by a circle of 10 cm diameter filling the field of view 306D. For this line, the measured signal exceeds the reconstructed one by $0.8 \cdot 10^6$ W/m$^2$ ($\pm 0.4 \cdot 10^6$ W/m$^2$ estimated). Interpreting the difference as heat flux from neutrals yields 1.3 MW of neutral loss. Since the poloidal cross-section of the emissivity area is more oblique than a circle (Fig. 5b), the horizontal diameter of the emitting area is about two times larger than the vertical one reducing the estimate of the power loss through neutrals in the divertor to 0.7 MW. The average energy per deuterium-atom is then 5 eV.

## 4. Simulation results

In order to find the spatial distribution of the neutral fluxes onto the divertor plates, a simulation with EDGE2D-NIMBUS [8] was used. This simulation matches the ion-saturation current onto the target plates and the neutral pressure measurement in the divertor. The time slice of the simulation is 18.0 s, which is when the detachment process has started but not completed yet.

The results for the neutral particle fluxes onto the divertor and their average energy are shown in Fig. 7.

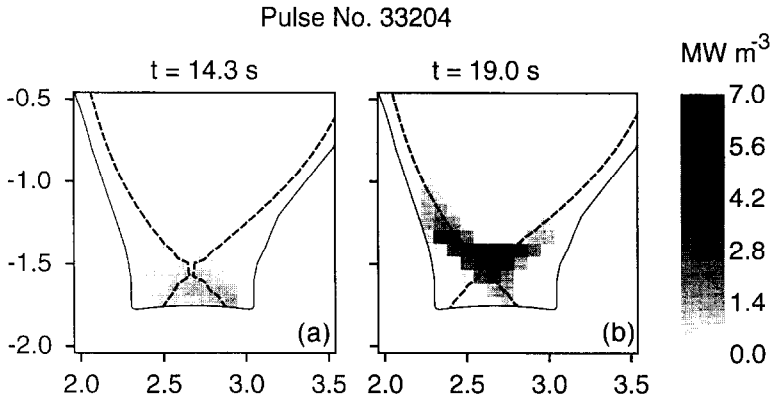


Fig. 5. Tomographic reconstruction of the radiation distribution in the (a) attached (14.3 s) and (b) the detached phase (19.0 s) of discharge 33204.

These are to be compared with the values estimated from the experimental data. The area of interest is the inner divertor, which is highlighted. The total flux $\Gamma_{\text{total}}$ of particles onto the wall segment in the field of view of the bolometer is $1\text{–}2 \cdot 10^{23}$ particle/(m$^2$ s). It is assumed that the particles are equally distributed into $2\pi$ below the wall segments surface. This gives an angular distribution $\Gamma_{\text{ang}}$ of

$$\Gamma_{\text{ang}} = \Gamma_{\text{total}}/2\pi = 0.16\text{–}0.32 \cdot 10^{23} \text{ particle}/(\text{m}^2 \text{ s sr}) \quad (1)$$

The detector sees of this flux only the small fraction $\Gamma_{\text{detector}}$ defined by its étendue $\varepsilon$

$$\varepsilon = F \cdot \Omega = 2.83 \cdot 10^{-8} \text{ m}^2 \text{ sr} \quad (2)$$

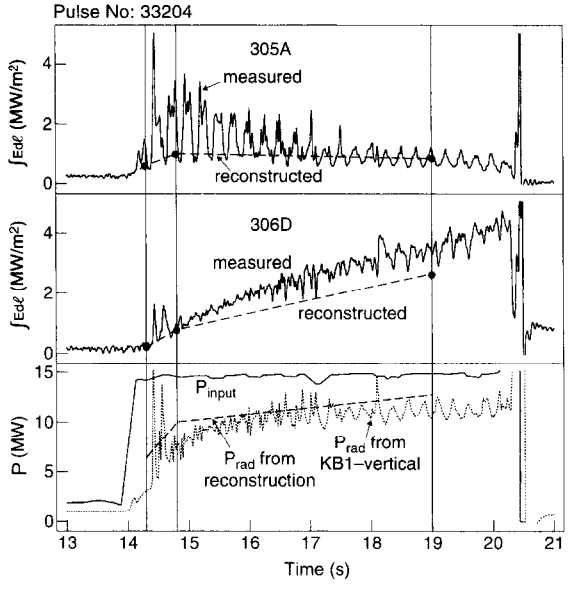


Fig. 6. Line of sight integrals of the radiation measured by 305A and 306D (see Fig. 1 for identification) in discharge 33204, total input power $P_{\text{input}}$ and total radiated power $P_{\text{rad}}$ calculated by using the vertical lines of sight of the old JET bolometer system KB1 (dotted line). Also shown are the results of tomographic reconstructions at 14.3 s, 14.8 s and 19.0 s taking all available bolometer measurements into account. As guide for the eye these results are joined by a broken line.

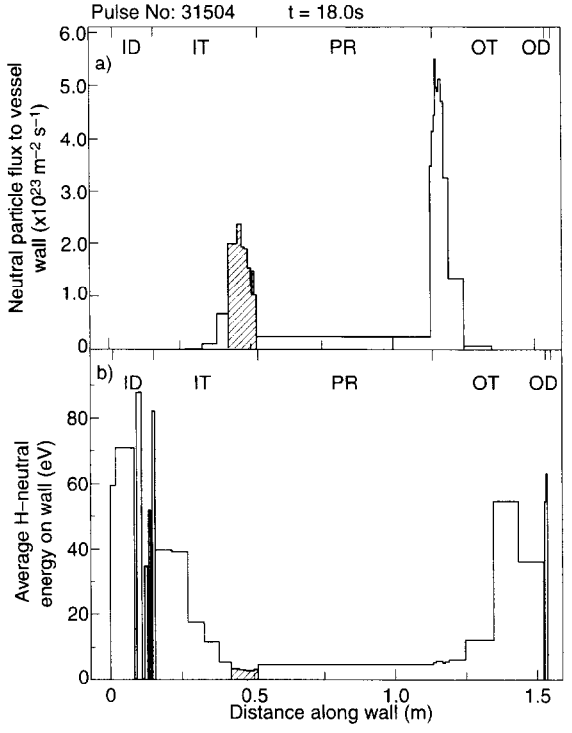


Fig. 7. (a) Neutral H-fluxes onto the vessel wall. PR is the private flux region, IT and OT are the inner and outer target regions ranging from. 5 cm inside of the separatrix, to 6 cm outside of the separatrix in outer mid-plane dimensions, ID and OD indicate the remaining part of the divertor outside the target area. Hatched is the area seen by the bolometer 305C. The $X$-axis is the poloidal distance along the wall starting at the innermost end of the divertor. (b) Average energies of neutral H-particles.

where $F$ is the detector area and $\Omega$ the solid angle:

$$\Gamma_{\text{detector}} = \Gamma_{\text{ang}} \cdot \varepsilon = 4.5\text{–}9.0 \cdot 10^{14} \text{ particle/s} \quad (3)$$

The total power received by bolometer 305C at a measured line integrated radiated power of $\int E\,dl = 0.6$ MW/m$^2$ is:

$$P = F \cdot \Omega \cdot \int E\,dl/4 \cdot \pi = 1.35 \cdot 10^{-3} \text{ W} \quad (4)$$

Using the particle flux onto the bolometer from modelling (Eq. (3)) and the measured power according to Eq. (4), the average energy $\langle W \rangle$ of the neutrals can be calculated. Assuming that half of the measured signal is due to neutral particle impact as suggested by the discrepancy between 305C and 409B in Fig. 4, this yields:

$$\langle W \rangle = P/\left(2 \cdot \Gamma_{\text{detector}} \cdot 1.6 \cdot 10^{-19} \text{ W s/eV}\right) = 4.6\text{–}9.4 \text{ eV} \quad (5)$$

Comparing this result with the simulation result (Fig. 7b) shows reasonable agreement, although being somewhat on the high side.

The total power that is contained in the neutral particle flux to the divertor wall is about 0.9 MW from the modelling.

## 5. Discussion

In this paper, the additional signal measured in the divertor is attributed to charge exchange neutrals. Part of this extra signal can be due to non-uniform radiation and differences in the respective observation areas near the target. The sweeping of the plasma over the line of sight of 305C can be used to unfold the non-uniform radial radiation profile at the inner strike zone (Fig. 8): 305C resolves the spatial variation of the radiation very well since its radial observation width at the target is only about 1.5 cm and the sweep amplitude is 5 cm. The other lines of sight, UPHC10, UPH9 and 409B, looking from the opposite site, have considerable larger viewing widths on the strike zone area as indicated in Fig. 8. They do not show much of the modulation due to the sweep. The light distribution is estimated by attempting to match the integral of the signal of the ex-divertor lines of sight to the shape suggested by 305C. At 14.6 s a match is not possible indicating a large neutral particle flux contribution. At 18 s the radiation profile could account for up to 85% of the signal level of channel 305C of electromagnetic radiation. This means that the average energy of 5–10 eV calculated earlier is an upper limit and the actual values that one can derive from the shaded area in Fig. 8 are in the range of 1.5–3 eV which envelops the simulation result of about 2.5 eV.

Other situations where power deposition by neutrals increase bolometer signals are described in [4] as: charge-exchange flux originating from a gas-puff next to a bolometer and warm gas, released from the wall after disruptions onto cooled bolometers.

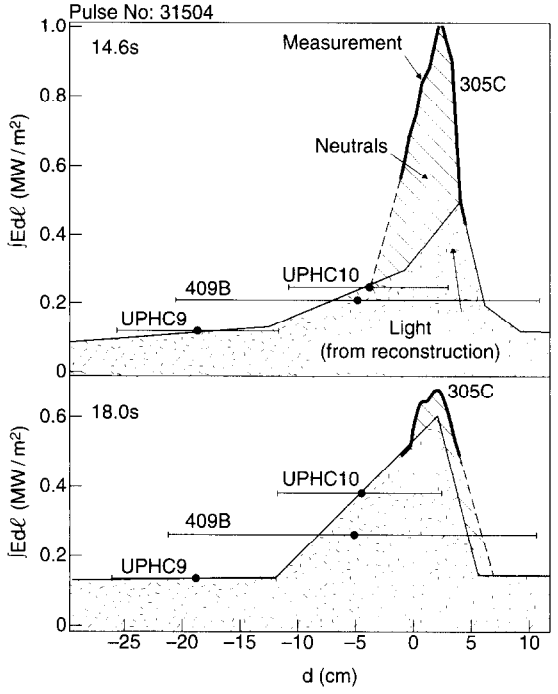


Fig. 8. Radiation profiles, separated into contributions from light (stippled area) and neutrals (hatched area). The $x$-axis is the distance $d$ from the inner divertor corner perpendicular to the inner divertor leg. 305C is unfolded utilising the sweep. The horizontal bars on the other lines of sight indicate the width of their respective detection area on the divertor surface (see Fig. 1 for identification).

Further possible influences of neutral gas on bolometer measurements are:

1. The change of calibration factors in a dense gas due to increased conductivity and
2. a strain gauge effect in the resistors.

These effects are still being studied [9], but based on the observed change of the calibration values by a factor 2–4 when going from vacuum to atmospheric pressure and the fact that Pirani pressure gauges, operating on the same principle, are down to a few percent of their full scale signal in the pressure range of interest (see e.g. [10]), it can be assumed that conductivity changes play no important role. The stiffness of the detector foil should also resist well any noticeable strain gauge effect in this pressure range.

The next generation tomography needs to include solid angle effects in order to test these findings more thoroughly and correct for them automatically. As a following step it may be possible to include an extra treatment of the neutrals by assuming that the sources of light radiation are also sources of neutrals, to which however the main plasma is not transparent.

Presently the simulation data give only the total flux to wall segments. As a next step, also its angular distribution

should become available thus removing another uncertainty in this analysis.

## 6. Conclusions

The excessive signal strength measured with the divertor bolometers can be explained as low energy neutral charge exchange particle fluxes. The average energy of the neutral particles reaching the inner strike zone while detachment is well under way is 1.5–3 eV from the bolometer analysis when taking finite line of sight effects into account and 2.5 eV from the simulation. When moving towards detachment the localised flux onto the strike zones is found to decrease and the charge exchange zone moves up to the X-point as well. The total power carried by the neutral losses is estimated to be of the order of 1 MW in JET's divertor.

## References

[1] V.S. Voitsenya et al., in: Diagnostics for Experimental Thermonuclear Fusion Reactors, eds. P.E. Stott, G. Gorini and E. Sindoni (Plenum Press, New York, 1996) pp. 61–66.
[2] K.F. Mast et al., Rev. Sci. Instrum. 56(5) (1985) 969.
[3] R. Reichle et. al., Proc. 22nd EPS Conf. on Controlled Fusion and Plasma Physics, Bournemouth, U.K., July 3–July 7, 1995 (The European Physical Society, 1995).
[4] R. Reichle et al., in: Diagnostics for Experimental Thermonuclear Fusion Reactors, eds. P.E. Stott, G. Gorini and E. Sindoni (Plenum Press, New York, 1996) pp. 560–563.
[5] R. Behrisch and W. Eckstein, in: Physics of Plasma–Wall Interactions in Controlled Fusion, eds. D.E. Post and R. Behrisch (Plenum Press, New York, 1986) pp. 413–438.
[6] W. Eckstein and J.P. Biersack, Appl. Phys. A 38 (1985) 123.
[7] J.C. Fuchs et al., Proc. 21st EPS Conf. on Controlled Fusion and Plasma Physics, Montpellier, France, June 27–July 1, 1994 (The European Physical Society, 1994).
[8] R. Simonini, G. Corrigan, G. Radford, J. Spence and A. Taroni, Contrib. Plasma Phys. 34 (1994) 368.
[9] K.F. Mast, private communication.
[10] D.R. Denison, in: Vacuum Physics and Technology, eds. G.L. Weissler and R.W. Carlson, Vol. 14 (Academic Press, New York 1979) p. 57.